Zero-doping state and electron-hole asymmetry in an ambipolar cuprate

Kouji Segawa,[1] M. Kofu,[2] S.-H. Lee,[2,*] I. Tsukada,[3] H. Hiraka,[4]
M. Fujita,[4] S. Chang,[5] K. Yamada,[6,†] and Yoichi Ando[1,‡]

[1]*Institute of Scientific and Industrial Research, Osaka University, Ibaraki, Osaka 567-0047, Japan*

[2]*Department of Physics, University of Virginia, Charlottesville, VA 22904-4714, USA*

[3]*Central Research Institute of Electric Power Industry, Yokosuka, Kanagawa 240-0196, Japan*

[4]*Institute for Materials Research, Tohoku University, Sendai, 980-8577, Japan*

[5]*NIST Center for Neutron Research, National Institute of Standards and Technology, Gaithersburg, MD 20899, USA*

[6]*Advanced Institute for Materials Research, Tohoku University, Sendai, 980-8577, Japan*

(Dated: January 19, 2010)

What exactly happens when a charge carrier is doped into a Mott insulator is a key question in many-body physics, for it lies at the heart of the problem of the high-temperature superconductivity in cuprates[1–4]. To address this issue, ideally one should start from a zero-doping state[5–7] and be able to introduce both holes and electrons in the dilute limit. However, such an idealized experiment has been impossible because of the lack of suitable materials. Here we show that a new "ambipolar" cuprate makes it possible for the first time to cross the zero-doping state in the same material, which in turn allows us to address physics of the extremely low doping region. Surprisingly, we found that the antiferromagnetic ground state sharply changes between electron- and hole-doped sides, and this change is dictated by the existence of only 0.1 ppm of charge carriers. Moreover, we observed that the Néel temperature T_N shows an unexpected reduction in a narrow range near the zero-doping state and, intriguingly, T_N is the highest for ∼10 ppm of hole doping. Our results indicate that the physics of the low doping region close to the Mott state is more intricate than expected, and call for a theoretical reexamination of the Mott physics.

Most of the cuprate superconductors are either uniquely hole-doped (p-type) as in $La_{2-x}Sr_xCuO_4$, $YBa_2Cu_3O_y$ (YBCO), and $Bi_2Sr_2CaCu_2O_{8+\delta}$, or electron-doped ($n$-type) as in $Ln_{2-x}Ce_xCuO_4$ (Ln = Nd, Pr). The main structural difference is the lack of apical oxygens in the n-type cuprates[4]. It was only recently (2006) that a system has been found where the sign of the charge carriers can be flipped without altering the crystal structure[8]. In $Y_{1-z}La_z(Ba_{1-x}La_x)_2Cu_3O_y$ (YLBLCO), the substitution of La for Ba provides electrons and, for $x = 0.13$ and $z = 0.62$, the charge carriers can be controlled[8] from 7% of holes per planar Cu (superconducting below 25 K) to 2% of electrons (non-superconducting) through the zero-doping state, by simply changing the oxygen content. Figure 1 shows the crystal structure and the scheme of chemical doping in YLBLCO, together with a generalized phase diagram of the cuprates. To the best of our knowledge, YLBLCO is so far the only *ambipolar* cuprate that provides a unique opportunity to investigate the extremely low doping region around the Mott insulating boundary spanning both p- and n-type regimes.

Let us begin by showing how the resistivity changes upon ambipolar doping. Figures 2a-2c show the temperature dependence of the c-axis resistivity, ρ_c, for various oxygen contents in YLBLCO from $y = 6.22$ to 6.80, measured up to 500 K. The highest value of ρ_c at room

temperature is achieved for $y = 6.32$: $\rho_c(300\ \mathrm{K}) \simeq 10^5\ \Omega$cm, which is unprecedented for cuprates. This suggests that the real boundary between n- and p-type cuprates which is defined as the Mott-insulating state is close to $y = 6.32$. ρ_c does not change much for $y =$ 6.31–6.36 (Fig. 2b), and it starts to decrease for $y < 6.31$ (Fig. 2c), which is due to the conductance of electron carriers[8].

Upon a close examination, one can notice that $\rho_c(T)$ exhibits a weak kink at each doping concentration. The anomaly can be seen more clearly, as either a peak or a dip, when the normalized temperature derivative of $\rho_c(T)$, $(d\rho/dT)/\rho$, is plotted in Figs. 2d-2f. The dip, observed in p-type samples with $y \geq 6.32$ (Figs. 2d-2e), is similar to the dip observed[9] in the pristine YBCO. On the other hand, in the n-type samples ($y \leq 6.30$) a *peak* rather than a dip is observed (Fig. 2f). Later, our neutron scattering data will show that the anomaly is associated with magnetic ordering. However, the different kinks suggest asymmetry between p- and n-type cuprates in the transport properties. Before we discuss doping dependence of the transport properties, let us discuss how the magnetic ground state evolves when the nature of the charge carriers changes near the Mott critical point, $y = 6.32$.

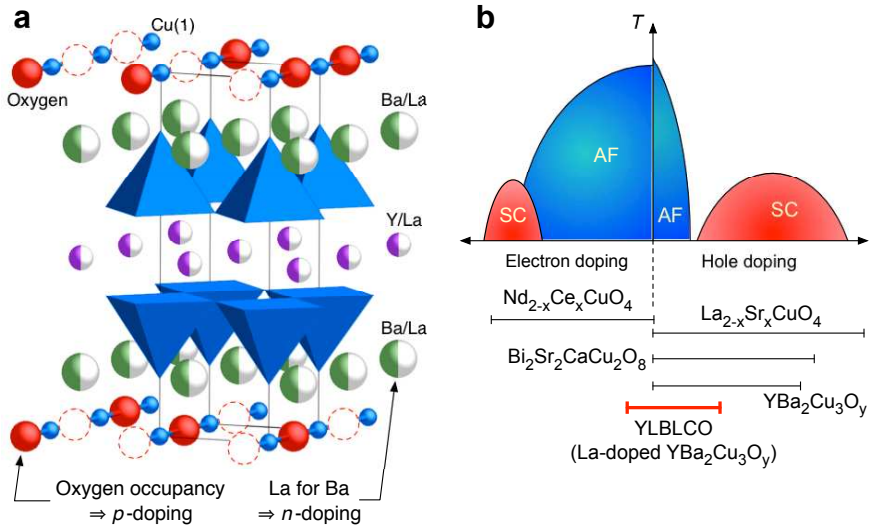

FIG. 1: **Schematics of YLBLCO. a**, Crystal structure of YLBLCO and the scheme of chemical doping. Note that in actual YLBLCO the Cu-O chains are fragmented and randomly oriented, leading to a macroscopically tetragonal structure. **b**, Generalized phase diagram of cuprate materials, where AF and SC denote antiferromagnetic and superconducting regions, respectively. Attainable doping ranges are shown for several cuprate materials including YLBLCO.

Elastic neutron scattering measurements were performed on the very same crystals as used in the $\rho_c(T)$ measurements. Figs. 3a-3f show the data taken along the (0.5, 0.5, L) direction centered at $L = 1$ and 1.5. For the electron-doped (n-type) sample with the oxygen content of $y = 6.22$, at 7 K a sharp peak exists at the half integer L (Fig. 3d), and no signal at the integer L (Fig. 3a). For the hole-doped (p-type) sample with $y = 6.69$, on the other hand, no peak was observed at the half integer L (Fig. 3f) and instead a peak appeared at the integer L (Fig. 3c). The magnetic ordering in both compositions occur at ∼370 K (Figs. 3g and 3i), which is consistent with the temperature where $\rho_c(T)$ and $\mathrm{d}\rho_c/\mathrm{d}T$ show the anomaly. The magnetic Bragg peaks were measured at several different corresponding wavevectors with half-integer Ls for $y = 6.22$ and with integer Ls for $y = 6.69$, and their relative intensities were used to determine their magnetic ground state structures. For both compositions, the Cu^{2+} moments at the Cu sites in the CuO_2 planes [called Cu(2)] are antiferromagnetically ordered in the ab-plane with an ordered moment $\langle M \rangle$ of 0.35(10)

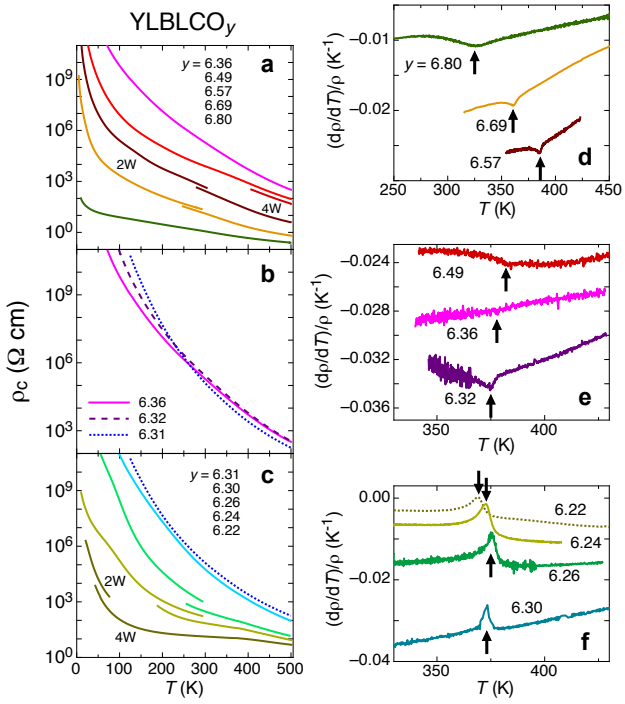

FIG. 2: **Temperature dependence of ρ_c. a-c**, $\rho_c(T)$ of in YLBLCO in semi-log plots, where "4W" (four-wire) and "2W" (two-wire) denote the methods for resistivity measurements. **d-f**, Temperature derivative of $\rho_c(T)$ normalized by ρ_c. The arrows indicate the position of the peak or the dip, at which the Néel transition is supposed to take place.

μ_B/Cu^{2+}, represented by red and blue spheres in the insets of Figs. 3a and 3d. The Cu-bilayers are coupled antiferromagnetically in both cases, and when translated by one lattice unit along the c-axis the moments change sign for the n-type while they are the same for the p-type. The moments at the Cu sites in the Cu-O-chain layers [called Cu(1)] were small or negligible: $\langle M \rangle_{\mathrm{Cu(1)}} = 0.05(2)\mu_B$/Cu and 0.00 μ_B/Cu for $y = 6.22$ and 6.69, respectively.

In order to confirm that the observed magnetic structures are the generic ground states for the n- and p-type YLBLCO and to study how one magnetic structure evolves into another when the oxygen concentration increases, we performed similar measurements on YLBLCO

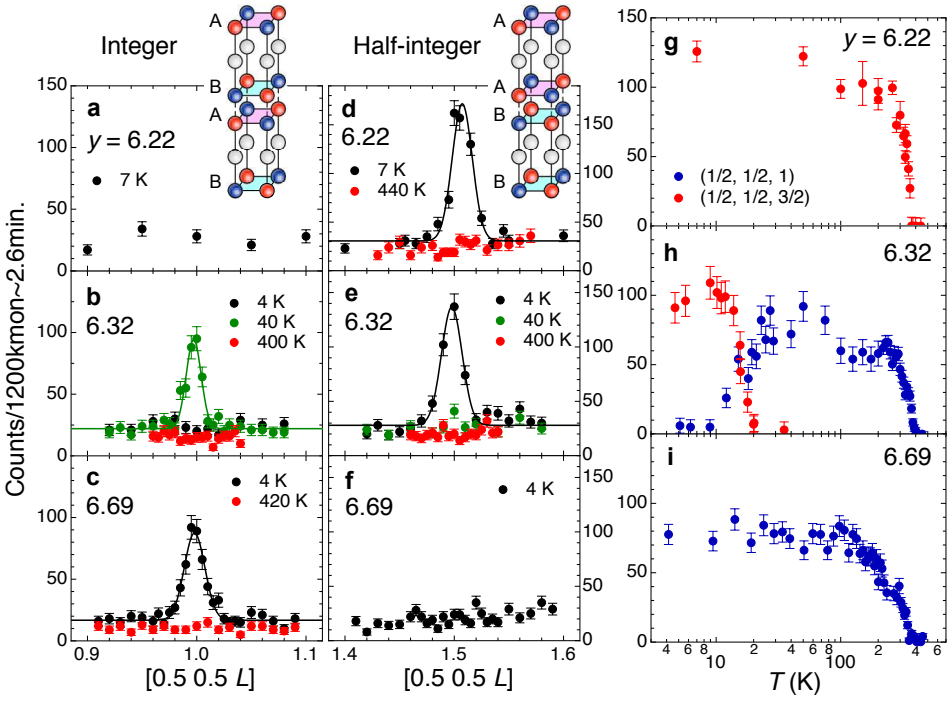

FIG. 3: **Magnetic ground states of YLBLCO studied by neutron scattering. a-f**, Neutron scattering intensities obtained by (0.5, 0.5, L) scans for (a,d) $y = 6.22$ (electron doped), (b,e) $y = 6.32$ (nearly zero doping) and (c,f) $y = 6.69$ (hole doped), at different temperatures. The insets show schematic pictures of the magnetic structures of YLBLCO for respective regimes. Red and blue spheres at the Cu(2) sites stand for spins with opposite directions (the spin easy axis lies in the plane, but the exact direction is unknown), while gray spheres are the Cu(1) atoms. The small (or negligible) moments of the Cu(1) atoms are not plotted. The letters A and B denote the difference (π-phase shift) in spin arrangements in the plane. **g,h,i**, Temperature dependences of the integrated intensity of the magnetic reflections for $y = 6.22$, 6.32, and 6.69.

($y = 6.32$). The oxygen content of $y = 6.32$ was chosen because this is the closest to the Mott critical point which separates the n- and p-type regions; indeed, the Hall coefficient R_H shows a sign change across this composition (see Fig. 4b). As shown in Figs. 3b, 3e and 3h, in this case upon cooling the integer L peak first develops below ∼370 K but upon further cooling it starts to decrease at ∼20 K below which the half-integer L peak appears. The ordered moments of the Cu(2) sites were 0.27(9) and 0.29(8) μ_B/Cu^{2+} for the half-integer L and the integer L phase, respectively, while those of the Cu(1) sites were 0.008(3) and 0.00 μ_B/Cu^{2+} for the half-integer L and the integer L phase, respectively. This crossover from the integer L to the half-integer L peak upon cooling probably indicates that the sign of the dominant charge carriers in the $y = 6.32$ sample changes at ∼20 K, although R_H could not be measured on this sample due to a very high impedance. This also indicates that the observed magnetic structures are indeed the generic ground states for the electron and hole doped YLBLCO.

What causes the magnetic ground state to change abruptly when the sign of the charge carrier changes? We can rule out any crystal structural origin because no abrupt change in the crystal structure including the lattice constants was found at the n-to-p-type crossover. Experimentally, it appears that the magnetic moments at the Cu(1) sites in the Cu-O-chain layers play a crucial role in selecting the particular magnetic ground state. For $y = 6.22$ (n-type), the small but nonzero moments at the Cu(1) planes would favor the observed $\mathbf{Q}_m = (0.5, 0.5, 0.5)$ magnetic structure along the c-axis if they are coupled antiferromagnetically with the neighboring Cu(2) layers. For $y = 6.69$ (p-type), on the other hand, the nonmagnetic Cu(1) layers would not have such an effect, leading to the observed $\mathbf{Q}_m = (0.5, 0.5, 1)$ magnetic structure. It is to be noted that the Cu(1) ions become magnetically ordered when excess electrons are doped rather than when excess holes are doped, even though the electron doping would decrease the number of magnetic Cu^{2+} ions (with nine $3d$ electrons) at the Cu(1) site[11].

In Fig. 4a, ρ_c is plotted as a function of the oxygen content at three different temperatures. It clearly shows that YLBLCO realizes the Mott-insulating state at $y \simeq 6.32$. When electrons are added or subtracted from this Mott state, ρ_c decreases but with a faster rate for n-type and a slower rate for p-type. The carrier concentration n_c calculated from the Hall coefficient R_H is plotted in Fig. 4b as a function of y, which confirms both the sign change of the main carriers near $y = 6.32$ and the different rate of charge transfer for the two regimes. Note that,

because the cuprates are charge-transfer-type Mott insulators, the electron doping involves a spectral-weight transfer from high energies and proceeds twice as quickly as the hole doping does in the localized limit[12]. It is interesting that the observed doping-rate asymmetry is qualitatively consistent with this picture.

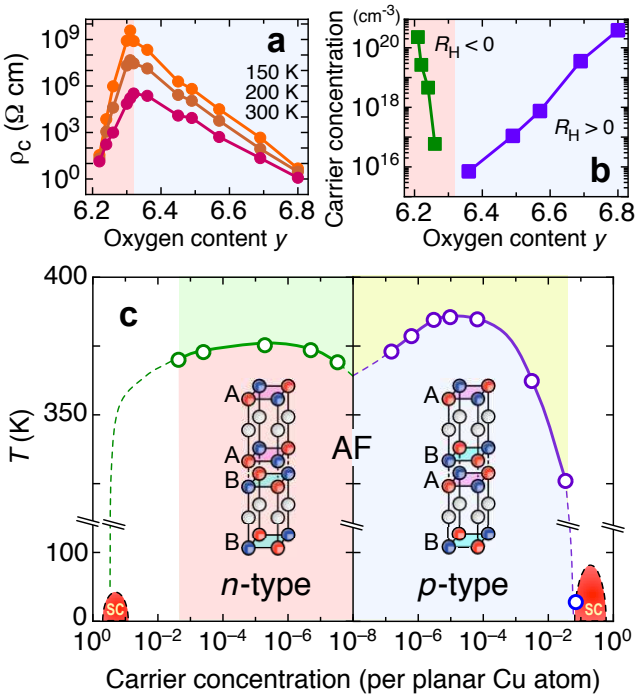

FIG. 4: **Evolution of key parameters in YLBLCO. a**, ρ_c presents a peak at $y = 6.32$, signifying the zero-doping point. **b**, The carrier concentration decreases exponentially towards the zero-doping point as y is varied; here, the R_H data at 300 K are used for the calculations, except for $y = 6.36$ and 6.49 for which 350 K data are used. Thin red and blue backgrounds denote the n- and p-type regimes, respectively. The carrier mobility along the c-axis calculated from these data is 10^{-3}–10^{-2} cm^2/Vs and is rather independent of both the concentration and the type of carriers. **c**, T_N as a function of the concentration of both p- and n-type carriers is shown (solid lines are guide to the eye), together with the anticipated phase boundary for the regimes not covered in this study (dashed lines). Note that the horizontal axes is plotted in a logarithmic scale, and the region studied here is highlighted with thin colours. T_N is extracted from the $\rho_c(T)$ data shown in Figs. 2d-2f. The carrier concentrations for $y = 6.30$, 6.31, and 6.32 are estimated from ρ_c by extrapolating the relation between ρ_c and R_H.

Fig. 4c shows the n_c-vs-T_N phase diagram of YLBLCO. In the n-type regime, the half-integer L magnetic state is stable over a very wide range of n_c spanning five orders of magnitude, with the maximum T_N at $n_c \sim 10^{-5}$ per planar Cu atom. When n_c approaches the zero-doping Mott-insulator point, T_N decreases. When the charge carrier becomes p-type, T_N starts increasing again as n_c increases up to $\sim 10^{-5}$ per planar Cu atom beyond which T_N decreases. The unexpected dip in T_N at the zero-doping point cannot be explained by a simple argument and obviously points to a new physics in the unexplored regime of very dilute carriers in Mott insulators. Also, the magnetic structure changes between p- and n-types in response to as small as 0.1 ppm of carriers, which is surprising. It seems that there is an unexpected "competition" between the two regimes, which leads to those intriguing phenomena near the zero-doping state.

In conclusion, we show that the ambipolar cuprate YLBLCO opens up an experimental opportunity to investigate the physics near the zero-doping state of Mott-insulating cuprates. Our study revealed some surprising features: the abrupt change of the magnetic structure by just 0.1 ppm of doping, the anomalous reduction of T_N near the zero-doping state, and the asymmetric behaviors in the transport properties. Clearly, the physics of very dilute carriers in Mott insulators is more intricate than expected[1–3], and its understanding may help disentangle the complex physics[13] of the cuprates.

Method:

Single crystals of $Y_{1-z}La_z(Ba_{1-x}La_x)_2Cu_3O_y$ (YLBLCO) are grown by a flux method using 99.9%-pure Y_2O_3 crucibles. The chemical composition of the grown crystals are analyzed by the inductively-coupled plasma atomic-emission spectroscopy, which gives $z = 0.62$ and $x = 0.13$. The carrier concentration in YLBLCO can be controlled from $\sim$2% of n-type carriers to $\sim$7% of p-type ones through the Mott insulator by changing the oxygen content y from 6.22 to 6.95 (ref. 8). Reducing y to below 6.22 results in decomposition of the crystal. ρ_c is measured by the four-wire method for resistance below $\sim$100 kΩ, and by the two-wire method for higher resistance up to $\sim 10^{11}$ Ω, where the Keithley 6517A electrometer is used with the guarding technique. All the measurements of ρ_c are performed on the same two crystals while varying the oxygen content; removable electrodes are used and the crystals are reannealed after each measurement. The error in the absolute value of the resistivity in the two crystals is within 20% for the four-wire method, and 50% for the two-wire method.

The Hall coefficient is measured by sweeping the magnetic field applied along the c-axis up to 7 T, and the error can be up to 20% for high resistance compositions. The elastic neutron scattering measurements were carried out on the cold neutron triple-axis spectrometer SPINS at the National Institute of Standards and Technology. The neutron energy was fixed to 3.7 meV. Contamination from higher-order beams was effectively eliminated using Be and BeO filters, before and after the sample whose size was $0.5\times0.5\times0.2$ mm^3.

Correspondence and requests for materials should be addressed to Y.A. or S.H.L. or K.Y.

Acknowledgments

We thank E. Dagotto, P. Phillips, and T. Tohyama for discussions. This work was supported by KAKENHI Grant Nos. 19674002, 20030004, 19340090, 19540358 and 20740196. Works at UVA and at NCNR were supported by the U.S. DOE (BES-DMSE) Award No. DE-FE02-07ER46384 and NSF Award No. DMR-0454672, respectively.

---

* Electronic address: shlee@virginia.edu

† Electronic address: kyamada@imr.tohoku.ac.jp

‡ Electronic address: y_ando@sanken.osaka-u.ac.jp

[1] Dagotto, E. Correlated electrons in high-temperature superconductors. *Rev. Mod. Phys.* **66**, 763-840 (1994).

[2] Lee, P. A., Nagaosa, N. & Wen, X.-G. Doping a Mott insulator: Physics of high-temperature superconductivity. *Rev. Mod. Phys.* **78**, 17-85 (2006).

[3] Phillips, P. Mottness. *Ann. Phys.* **321**, 1634-1650 (2006).

[4] Imada, M., Fujimori, A. & Tokura, Y. Metal-insulator transitions. *Rev. Mod. Phys.* **70**, 1039-1263 (1998).

[5] Kastner, M. A., Birgeneau, R. J., Shirane, G. & Endoh, Y. Magnetic, transport, and optical properties of monolayer copper oxides. *Rev. Mod. Phys.* **70**, 897-928 (1998).

[6] Basov, D. N. & Timusk, T. Electrodynamics of high-T_c superconductors. *Rev. Mod. Phys.* **77**, 721-779 (2005).

[7] Ono, S., Komiya, S. & Ando, Y. Strong charge fluctuations manifested in the high-temperature Hall coefficient of high-T_c cuprates. *Phys. Rev. B* **75**, 024515 (2007).

[8] Segawa, K. & Ando, Y. Doping n-type carriers by La-substitution for Ba in $YBa_2Cu_3O_y$ system. *Phys. Rev. B* **74**, 100508 (2006).

[9] Lavrov, A. N., Ando, Y., Segawa, K. & Takeya, J. Magnetoresistance in heavily underdoped $YBa_2Cu_3O_{6+x}$: antiferromagnetic correlations and normal-state transport. *Phys. Rev. Lett.* **83**, 1419-1422 (1999).

[10] Tranquada, J. M. *et al.* Neutron-diffraction determination of antiferromagnetic structure of Cu ions in $YBa_2Cu_3O_{6+x}$ with x =0.0 and 0.15. *Phys. Rev. Lett.* **60**, 156-159 (1988).

[11] Jorgensen, J. D. *et al.* Structural properties of oxygen-deficient $YBa_2Cu_3O_{7-\delta}$. *Phys. Rev. B* **41**, 1863-1877 (1990).

[12] Meinders, M. B., Eskes, H. & Sawatzky, G. A. Spectral-weight transfer: Breakdown of low-energy-scale sum rules in correlated systems. *Phys. Rev. B* **48**, 3916-3926 (1993).

[13] Bonn, D. A. Are high-temperature superconductors exotic? *Nat. Phys.* **2** 159-168 (2006).

Supplementary Information

Previous observation of the n-type magnetic structure: It is interesting to note that the present result of the magnetic ground state for the near-zero-doping sample ($y = 6.32$), including the temperature-induced crossover, is very similar to that observed in heavily oxygen-deficient YBCO by Kadowaki *et al.* [S1]; in the light of the present work, it is possible that they had almost realized the zero-doping state in pristine YBCO crystals. Also, the result in $NdBa_2Cu_3O_{6.1}$ reported by Moudden *et al.* [S2] is rather similar, though only the *n*-type structure was observed below 385 K in $NdBa_2Cu_3O_{6.1}$; in this case, since it is well known that Nd atoms tend to substitute for the Ba sites, an electron-doped state may have been accidentally realized.

[S1] Kadowaki, H. *et al.* Successive magnetic phase transitions in tetragonal $YBa_2Cu_3O_{6+x}$. *Phys. Rev. B* **37**, 7932-7935 (1988).
[S2] Moudden, A. H. *et al.* Antiferromagnetic ordering of Cu ions in $NdBa_2Cu_3O_{6.1}$. *Phys. Rev. B* **38**, 8720-8723 (1988).